Journal of Power Sources 204 (2012) 85–88

Contents lists available at SciVerse ScienceDirect

Journal of Power Sources

journal homepage: www.elsevier.com/locate/jpowsour

Short communication

"Naked" Pd nanoparticles supported on carbon nanodots as efficient anode catalysts for methanol oxidation in alkaline fuel cells

Wentao Wei[a,b], Wei Chen[a,*]

[a] State Key Laboratory of Electroanalytical Chemistry, Changchun Institute of Applied Chemistry, Chinese Academy of Sciences, Changchun 130022, Jilin, China
[b] School of Chemistry & Environmental Engineering, Changchun University of Science & Technology, Changchun 130022, China

ARTICLE INFO

Article history:
Received 3 November 2011
Received in revised form
27 December 2011
Accepted 1 January 2012
Available online 9 January 2012

Keywords:
Electrocatalysis
Nanoparticle
Methanol oxidation
Palladium
Alkaline fuel cell
Carbon nanodots

ABSTRACT

Well-dispersed Pd nanoparticles supported on carbon nanodots are synthesized successfully with a facile and green method without any additional surfactant and reductant. The synthesized Pd–C hybrid nanoparticles provide high electrical conductivity and non-blocked active surfaces for organic molecular fuels oxidation. Compared to the commercial Pd/C catalysts, the present Pd–C hybrid nanocomposites exhibit more negative onset potential and much higher current density for methanol oxidation in alkaline media. The excellent electrocatalytic performance displayed in the electrochemical measurements indicates that such "naked" Pd nanoparticles have potential applications as promising anode catalysts in alkaline fuel cells.

© 2012 Elsevier B.V. All rights reserved.

1. Introduction

Direct liquid fuel cells, such as direct methanol fuel cells (DMFCs) and direct formic acid fuel cells (DFAFCs), represent one of the most effective candidates of clean power sources with high energy efficiency, high power density, low environmental pollution, and their ease of handling [1,2]. Of these, DMFCs have been found to have wide range of applications in potable electronic devices, transportation vehicles and power sources for space shuttles, factories and buildings [3]. Due to the high catalytic activity, platinum-based materials are often used as both anode and cathode electrocatalysts. However, the high-cost and the heavy CO self-poisoning of platinum catalysts hinder their wide-spread applications in fuel cells. One of the key challenges to the practical application and commercialization of fuel cells is the development and design of stable, highly active and low cost electrocatalysts. To this end, various Pt-based and Pt-free nanomaterials have been investigated extensively in the past decade [4–6].

Among the studied non-Pt catalysts, palladium and Pd-based nanomaterials are the promising alternatives on both anode and cathode sides [7–10]. In recent years, extensive investigations have showed that the Pd-based nanostructured materials exhibit high electrocatalytic activities towards organic small molecules oxidation with low CO poisoning during the reactions [11]. In practical fuel cell applications, the metal catalysts are usually dispersed on supports with high electrical conductivity and high stability. Various carbon materials including traditional carbon black and novel carbon nanomaterials, such as carbon nanotubes [12], carbon nanofibers [13], graphene [14,15], fullerenes [16], and tungsten carbide [17] have been employed as promising supports for metal catalysts. Another novel carbon-based nanomaterial, carbon nanodots are attracting much attention because of their unique electronic, optical and thermal properties, and variety of potential applications. In the previous studies, micrometer- and nanometer-sized spheres have been used as catalysts support materials [18–21]. In these investigations, the sizes of the carbon spheres are larger than 100 nm and the metal nanoparticles were usually deposited on the surfaces of carbon spheres by reducing metal salts with reducing agents, such as sodium borohydride [18,20], ascorbic acid [22], sodium hydrosulfite [19], and polyols [19].

In the present communication, we demonstrate that naked and well-dispersed Pd nanoparticles supported on carbon nanodots (CN-PdNPs) were successfully prepared with a green synthetic rout. Different from the previous reports, no additional reductants and surfactants were used for the synthesis of Pd nanoparticles. It was found that the freshly prepared carbon nanodots themselves can act as reductants for metal nanoparticles formation on their surfaces. More importantly, such non-surfactant capped metal nanoparticles provide naked catalytic surfaces, which renders them

* Corresponding author. Tel.: +86 431 85262061; fax: +86 431 85262697.
E-mail address: weichen@ciac.jl.cn (W. Chen).

0378-7753/$ – see front matter © 2012 Elsevier B.V. All rights reserved.
doi:10.1016/j.jpowsour.2012.01.032

the highly active electrocatalysts for fuel cells. As expected, the CN-PdNPs exhibit high electrocatalytic activity for methanol oxidation in alkaline media.

2. Experimental

2.1. Chemicals

D-Glucose, methanol (CH_3OH), and palladium chloride ($PdCl_2$) were purchased from Beijing Chemical Reagent. Commercial palladium catalyst, 5% on activated carbon powder (nominally 50% water wet) and Nafion solution (5 wt%) were purchased from Alfa Aesar. All chemicals were used as received without further purification. Water was supplied by a Water Purifier Nanopure water system (18.3 MΩ cm).

2.2. Synthesis of carbon nanodots

The carbon nanodots were synthesized according to the modified procedure described by Sun and Li [21]. In a typical procedure, 0.2973 g glucose was dissolved in 15 mL Nanopure water, followed by stirring and ultrasonication forming a homogeneous and clear solution, which was then placed in a 20 mL autoclave with a Teflon seal and maintained at 180 °C for 4–8 h. The products were then cooled to room temperature naturally. The precipitates were collected by centrifugation and then rinsed with Nanopure water and alcohol for three times, respectively. Ultrasonic operation was used to re-disperse the precipitates during the rinsing process. Finally, the carbon nanodots were separated for further characterizations.

2.3. Synthesis of carbon nanodots-supported palladium nanoparticles (CN-PdNPs)

5 mL of an aqueous suspension of carbon nanodots was heated at 100 °C under reflux for 10 min and then $0.0177 \times g$ $PdCl_2$ dissolved in water was added drop by drop under vigorous stirring. The suspension was refluxed for 30 min and then centrifuged, washed with Nanopure water and ethanol several times, and dried at 60 °C for 8 h.

2.4. Characterization

The size and the aggregation status of the carbon nanodots and CN-PdNPs were examined by using Hitachi H-600 transmission electron microscopy (TEM) operated at 100 kV. High-resolution TEM (HRTEM) measurements were carried out on a JEM-2010 (HR) microscope operated at 200 kV. Powder X-ray diffraction (XRD) was performed on a PW1700 Powder Diffractometer using Cu Kα radiation with a Ni filter (λ = 0.154059 nm at 30 kV and 15 mA). X-ray photoelectron spectroscopy (XPS) measurements were performed by using a VG Thermo ESCALAB 250 spectrometer (VG Scientific) operated at 120 W.

2.5. Electrochemistry

Prior to the deposition of the CN-PdNPs onto an electrode surface for electrocatalytic assessment, a glassy carbon (GC) electrode (3.0 mm in diameter) was polished with alumina slurries (0.05 μm) and cleansed by sonication in 0.1 M HNO_3, H_2SO_4 and pure water for 10 min successively. The dried CN-PdNPs were dispersed ultrasonically in Nanopure water and 5 wt% Nafion solution. After the ink formed homogeneously, a certain amount of the catalyst ink was then dropped on the clean GC electrode with a micropipette and then dried in vacuum at room temperature. The prepared electrode was denoted as CN-PdNPs/GC. The commercial Pd/C catalyst electrode was prepared with the same procedure.

Voltammetric measurements were carried out with a CHI 750D electrochemical workstation. The CN-PdNPs/GC electrode prepared above was used as the working electrode. A Ag/AgCl (in 3 M NaCl, aq.) and a Pt coil were used as the reference and counter electrodes, respectively. All electrode potentials in the present study were referred to this Ag/AgCl reference. All electrochemical experiments were carried out at room temperature.

3. Results and discussion

3.1. Synthesis and characterization of materials

The morphology of the synthesized carbon nanodots and CN-PdNPs was firstly characterized with TEM. Fig. 1(a) shows the TEM micrograph of the carbon nanodots. It can be seen that the carbon nanodots synthesized with hydrothermal method consist of homogeneous carbon nanospheres with the average size of 41.3 ± 4.5 nm. After the refluxing of carbon nanodots and palladium chloride, the well-dispersed Pd nanoparticles supported on carbon nanodots can be observed from the TEM image shown in Fig. 1(b) and (c). The average size of CN-PdNPs increases to 45.1 ± 5.9 nm. The surface structure of the CN-PdNPs was characterized with HRTEM (Fig. 1(d)), from which highly crystalline Pd nanocrystals with apparently resolved lattice fringes were formed on the amorphous carbon nanodots. The interplanar spacing of the lattice fringes could be ascribed to the (1 1 1) planes of palladium. The electron micrographs indicate that with the present synthesis method, Pd nanocrystals can be formed on the carbon nanodots surface although no additional reducing agent was added. Recently, it was also found that graphene oxide (GO) can also be used as reductant to prepare Pd nanoparticles anchored on the GO surfaces [14]. In the study, it was proposed that the functional groups on the surface of carbon materials play an important role in the spontaneous formation of metal nanoparticles. Actually, the previous FTIR studies have shown that abundant functional groups are present in the carbon nanoparticles synthesized with the similar route to our study [21]. The vibrational peaks corresponding to C—OH, C=C, C=O, *etc*. can be observed clearly. As proposed in the previous studies, the formation of Pd nanocrystals can be attributed to the direct redox reaction between carbon nanodots and Pd^{2+} ions [14,23]. It should be noted that in order to prepare carbon-supported Pd catalysts, complicated treatments were often needed to remove the protecting ligands bound on Pd nanoparticle surfaces [24]. So the present study provides a facile method to synthesize "naked" Pd nanoparticles on supports as efficient anode catalyst in alkaline fuel cells.

Fig. 2(a) shows the XRD patterns of the synthesized carbon nanodots and CN-PdNPs. From the pattern of carbon nanodots, a broad peak centered at 24.85° was observed, suggesting that the synthesized carbon material was amorphous. However, for the CN-PdNPs, except for the broad peak from amorphous carbon, strong diffraction peaks at 39.85°, 46.48°, 67.95° and 81.80° were observed, which could be indexed to the (1 1 1), (2 0 0), (2 2 0) and (3 1 1) facets of the Pd with face-centered-cubic (fcc) lattice crystal structure. The diffraction peaks from the CN-PdNPs agree well with the standard diffraction data of bulk palladium shown with green bars in Fig. 2. Note that the strongest diffraction peak is from Pd (1 1 1), which was found to be a very active facet for organic small molecules oxidation [25,26]. Therefore, the synthesized CN-PdNPs are structurally favored anode electrocatalysts for fuel cells. The average size of the Pd nanoparticles can be evaluated by the Debye–Scherrer equation, $D = k\lambda/\beta \cos\theta$, where D is the diameter of the nanoparticles, k is the shape factor (0.90), λ(Cu Kα) = 1.54059 Å, and β is the full width at half maximum of the diffraction peaks [27]. Based on the (1 1 1) diffraction peak shown in Fig. 2(a), the average diameter of the Pd nanoparticles was calculated to be 15.7 nm. It should be pointed

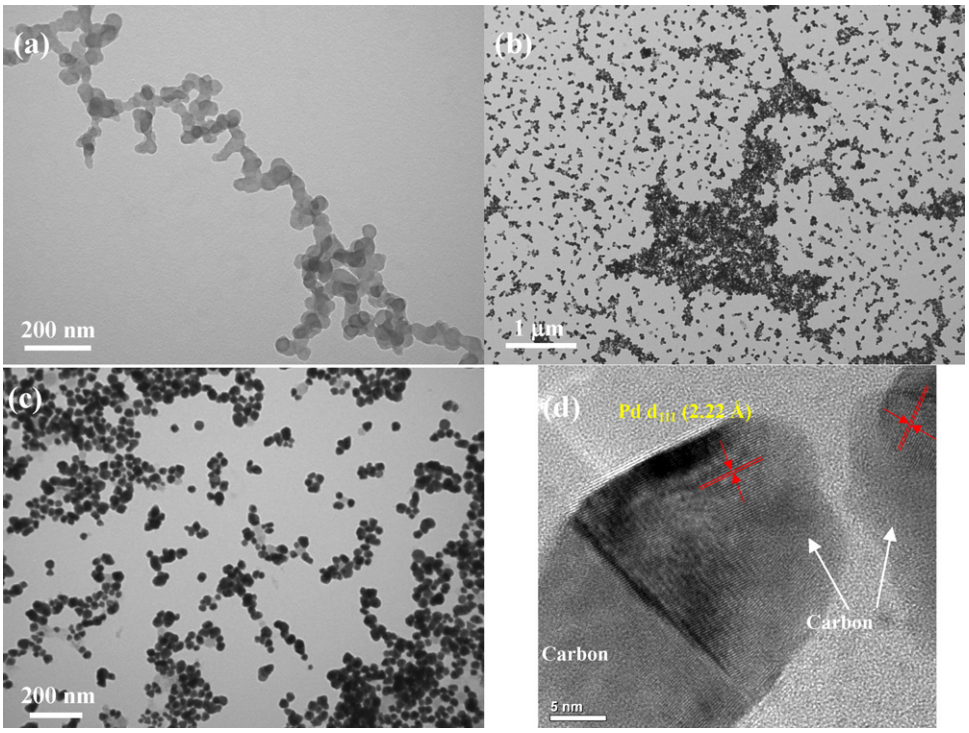

Fig. 1. (a) TEM micrograph of carbon nanodots; (b and c) TEM images with different magnifications and (d) HRTEM micrograph of the synthesized Pd nanoparticles supported on carbon nanodots.

out that the average size of CN-PdNPs (45.1 ± 5.9 nm) obtained from TEM measurements include the sizes of carbon nanodots and the deposited Pd nanoparticles. The chemical composition and the oxidation states of Pd nanoparticles were also examined with XPS measurements (the survey spectra are shown in Supporting Information, Fig. S1). Fig. 2(b) shows the Pd 3d XPS region, where the two strong peaks at 335.08 and 340.37 eV could be assigned to $3d_{5/2}$ and $3d_{3/2}$ of metallic Pd (0), respectively. The C 1s signal from the carbon nanodots can also be observed as shown in Fig. 2(c). In the Raman spectra (Supporting Information, Fig. S2) of the CN-PdNPs obtained at different points, the strong G band was observed at 1587 cm^{-1}, which can be attributed to the in-plane vibration of sp^2 carbon.

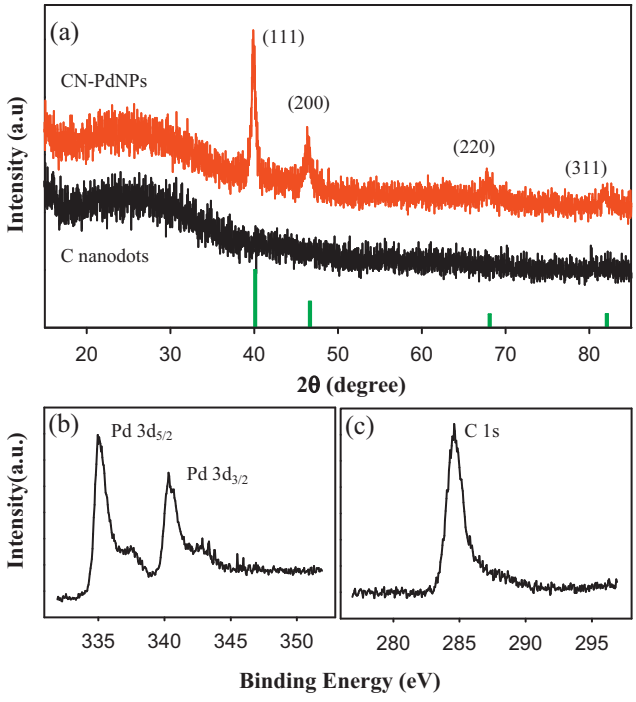

Fig. 2. (a) XRD patterns of the as-synthesized carbon nanodots and CN-PdNPs along with the bulk XRD pattern of Pd (green bars, from JCPDS No. 65-2867); (b) Pd 3d and (c) C 1s XPS spectra. (For interpretation of the references to color in this figure caption, the reader is referred to the web version of the article.)

3.2. Methanol electro-oxidation in alkaline electrolyte

The electrocatalytic activity of the synthesized CN-PdNPs for methanol oxidation in alkaline media was studied by cyclic voltammetry (CV). The CV of CN-PdNPs/GC electrode in 1 M KOH was shown in Fig. 3. In the low potential region, there is a pair of current peaks corresponding to the hydrogen desorption and adsorption on the Pd nanoparticles. In the negative-going potential sweep, an

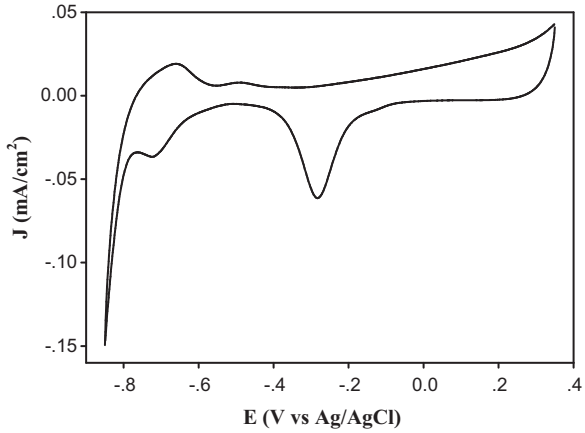

Fig. 3. Steady-state cyclic voltammogram of CN-PdNPs/GC electrode in 1 M KOH. Potential scan rate 20 mV s^{-1}.

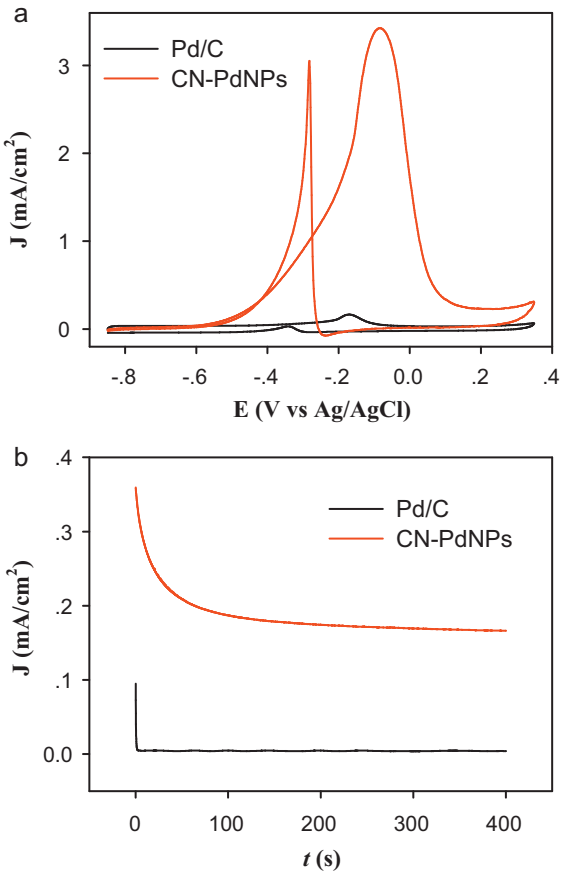

Fig. 4. (a) Cyclic voltammograms (CVs) and (b) chronoamperometric curves at −0.40 V of the synthesized Pd nanoparticles supported on carbon nanodots (red lines) and commercial Pd/C catalysts in 1 M CH_3OH + 1 M KOH solution. Potential scan rate in CVs is 20 mV s^{-1}. (For interpretation of the references to color in this figure caption, the reader is referred to the web version of the article.)

obvious reduction current peak at −0.28 V could be ascribed to the reduction of palladium oxides, which were formed at high potentials in the positive-going potential sweep. The observation of CV features from Pd indicates that the Pd nanoparticles supported on carbon nanodots exhibit high electrochemical activity although no post-synthesis treatment was applied to the CN-PdNPs. Fig. 4(a) depicts the CVs of methanol oxidation at CN-PdNPs (red curve) and commercial Pd/C catalysts (black curve) in 1 M CH_3OH + 1 M KOH with potential scan rate of 20 mV s^{-1}. On both electrodes, the voltammetric currents have been normalized to the electrochemically active surface areas (ECASA) based on the oxygen adsorption measurement method proposed by Trasatti and Petrii [28]. The anode peak current density of methanol oxidation on CN-PdNPs/GC is 3.42 mA cm^{-2}, which is 20 times higher than that obtained on commercial Pd/C catalysts. The catalytic activities can also be compared based on the onset potentials of methanol oxidation. From the CVs in Fig. 4(a), the onset potentials can be measured to be −0.62 and −0.54 V on CN-PdNPs and Pd/C, respectively. Such result means that the onset potential on CN-PdNPs is 80 mV more negative than that from the commercial catalysts. Both current density and onset potential of methanol oxidation demonstrate that the prepared CN-PdNPs exhibit much better catalytic performance than the commercial Pd catalysts. The electrochemical stability of the CN-PdNPs and Pd/C catalysts for methanol oxidation was compared with chronoamperometric measurements at −0.40 V (Fig. 4(b)). It can be seen that both initial and steady-state oxidation current densities at CN-PdNPs/GC are much larger than those from commercial one over the entire time period examined. More importantly, the current density decay on CN-PdNPs is significantly slower than that on Pd/C. At CN-PdNPs/GC electrode, the current density at the 400 s test is about 46.1% of the initial value, whereas only 4.0% of the initial current density maintained at the Pd/C catalysts. These electrochemical studies strongly indicate that the carbon nanodots-supported Pd nanoparticles exhibit enhanced electrochemical stability for methanol oxidation in alkaline electrolyte.

4. Conclusion

"Naked" Pd nanoparticles supported on carbon nanodots were synthesized with a facile and green method with the pre-synthesized carbon nanodots as reductants. The structural characterizations showed that the synthesized Pd nanoparticles are well-dispersed on the surfaces of carbon nanodots although no capping agent was present. As shown in the electrochemical studies, such Pd–C hybrid nanoparticles provide high electrical conductivity and non-blocked active surfaces for organic molecular fuels oxidation, which renders them the promising anode catalysts for alkaline fuel cells.

Acknowledgments

This work was supported by the National Natural Science Foundation of China (No. 21043013) and the startup funds for scientific research, Changchun Institute of Applied Chemistry, Chinese Academy of Sciences.

Appendix A. Supplementary data

Supplementary data associated with this article can be found, in the online version, at doi:10.1016/j.jpowsour.2012.01.032.

References

[1] C. Lamy, A. Lima, V. LeRhun, F. Delime, C. Coutanceau, J.M. Leger, J. Power Sources 105 (2002) 283–296.
[2] E. Antolini, J. Power Sources 170 (2007) 1–12.
[3] R.A. Lemons, J. Power Sources 29 (1990) 251–264.
[4] Y.Z. Lu, W. Chen, Chem. Commun. 47 (2011) 2541–2543.
[5] W. Chen, J. Kim, S.H. Sun, S.W. Chen, Phys. Chem. Chem. Phys. 8 (2006) 2779–2786.
[6] W. Chen, S.W. Chen, Angew. Chem.: Int. Ed. 48 (2009) 4386–4389.
[7] E. Antolini, Energy Environ. Sci. 2 (2009) 915–931.
[8] R. Larsen, S. Ha, J. Zakzeski, R.I. Masel, J. Power Sources 157 (2006) 78–84.
[9] W.P. Zhou, A. Lewera, R. Larsen, R.I. Masel, P.S. Bagus, A. Wieckowski, J. Phys. Chem. B 110 (2006) 13393–13398.
[10] Y.Z. Lu, W. Chen, J. Phys. Chem. C 114 (2010) 21190–21200.
[11] C. Bianchini, P.K. Shen, Chem. Rev. 109 (2009) 4183–4206.
[12] Z.Q. Tian, S.P. Jiang, Y.M. Liang, P.K. Shen, J. Phys. Chem. B 110 (2006) 5343–5350.
[13] K.M. Metz, D. Goel, R.J. Hamers, J. Phys. Chem. C 111 (2007) 7260–7265.
[14] X.M. Chen, G.H. Wu, J.M. Chen, X. Chen, Z.X. Xie, X.R. Wang, J. Am. Chem. Soc. 133 (2011) 3693–3695.
[15] S.J. Guo, S.J. Dong, E.W. Wang, ACS Nano 4 (2010) 547–555.
[16] H.W. Kroto, J.R. Heath, S.C. Obrien, R.F. Curl, R.E. Smalley, Nature 318 (1985) 162–163.
[17] F.P. Hu, P.K. Shen, J. Power Sources 173 (2007) 877–881.
[18] C.W. Xu, L.Q. Cheng, P.K. Shen, Y.L. Liu, Electrochem. Commun. 9 (2007) 997–1001.
[19] R.Z. Yang, X.P. Qiu, H.R. Zhang, J.Q. Li, W.T. Zhu, Z.X. Wang, X.J. Huang, L.Q. Chen, Carbon 43 (2005) 11–16.
[20] X. Wang, C.G. Hu, Y.F. Xiong, H. Liu, G.J. Du, X.S. He, J. Power Sources 196 (2011) 1904–1908.
[21] X.M. Sun, Y.D. Li, Angew. Chem.: Int. Ed. 43 (2004) 597–601.
[22] L. Tian, D. Ghosh, W. Chen, S. Pradhan, X.J. Chang, S.W. Chen, Chem. Mater. 21 (2009) 2803–2809.
[23] H.C. Choi, M. Shim, S. Bangsaruntip, H.J. Dai, J. Am. Chem. Soc. 124 (2002) 9058–9059.
[24] V. Mazumder, S.H. Sun, J. Am. Chem. Soc. 131 (2009) 4588–4589.
[25] W.J. Zhou, J.Y. Lee, J. Phys. Chem. C 112 (2008) 3789–3793.
[26] N. Hoshi, K. Kida, M. Nakamura, M. Nakada, K. Osada, J. Phys. Chem. B 110 (2006) 12480–12484.
[27] W. Chen, D. Ghosh, S.W. Chen, J. Mater. Sci. 43 (2008) 5291–5299.
[28] S. Trasatti, O.A. Petrii, Pure Appl. Chem. 63 (1991) 711–734.